

March 29, 2024
Revised: July 31, 2024



Sierra Nevada Work Unit 11, California Lidar Technical Data Report

Contract #: 140G0221D0012 Work Package #: 224823 Work Unit #: 300459

Prepared For:



United States Geological Survey
tnm_help@usgs.gov

Prepared By:



NV5 Corvallis
1100 NE Circle Blvd, Ste. 126
Corvallis, OR 97330
PH: 541-752-1204

TABLE OF CONTENTS

INTRODUCTION	1
Deliverable Products	2
ACQUISITION	5
Planning.....	5
Airborne Lidar Survey.....	7
Ground Survey.....	9
Base Stations.....	9
Ground Survey Points (GSPs).....	11
Land Cover Class	12
PROCESSING	14
Boresight Calibration.....	14
GNSS-Inertial Processing	14
Deliverables Processing.....	15
Feature Extraction.....	18
Hydroflattening and Water’s Edge Breaklines.....	18
Swath Separation Raster Processing	20
RESULTS & DISCUSSION.....	21
Lidar Density.....	21
Lidar Accuracy Assessments.....	24
Lidar Non-Vegetated Vertical Accuracy.....	24
Lidar Vegetated Vertical Accuracies	27
Lidar Relative Vertical Accuracy	29
Intraswath Precision (Smooth Surface Precision)	30
Lidar Horizontal Accuracy.....	30
CERTIFICATIONS	31
GLOSSARY	32
APPENDIX A - ACCURACY CONTROLS	33

Cover Photo: A view looking north at a dam and reservoir in the Work Unit 11 area of interest. The image was created from the lidar bare earth model overlaid with Virtual Earth imagery.

LIST OF FIGURES

Figure 1: Location map of the Sierra Nevada site in California.....	3
Figure 2: Location map of the Sierra Nevada Work Unit 11 site in California	4
Figure 3: Work Unit 11 flightlines map	8
Figure 4: Work Unit 11 ground survey location map.....	13
Figure 5: Example of hydroflattening in the Sierra Nevada Lidar dataset.....	19
Figure 6: Example of hydroflattening treatment applied to a reservoir with temporal water surface variation within the Sierra Nevada Lidar dataset	19
Figure 7: The color ramp values used in the Sierra Nevada project.....	20
Figure 8: Frequency distribution of first return point density values per 100 x 100 m cell	22
Figure 9: Frequency distribution of ground-classified return point density values per 100 x 100 m cell ..	22
Figure 10: First return and ground point density map for the Sierra Nevada Work Unit 11 site (100 m x 100 m cells)	23
Figure 11: Frequency histogram for lidar classified LAS deviation from ground check point values (NVA)	25
Figure 12: Frequency histogram for the lidar bare earth DEM surface deviation from ground check point values (NVA).....	26
Figure 13: Frequency histogram for the lidar surface deviation from ground control point values	26
Figure 14: Frequency histogram for the lidar surface deviation from vegetated check point values (VVA)	28
Figure 15: Frequency histogram for the lidar bare earth DEM deviation from vegetated check point values (VVA)	28
Figure 16: Frequency plot for relative vertical accuracy between flightlines.....	29

LIST OF TABLES

Table 1: Acquisition dates, acreage, and data types collected on the Sierra Nevada site	1
Table 2: Deliverable product projection information	2
Table 3: Products delivered to UCSD & USGS for the Sierra Nevada Work Unit 11 site	2
Table 4: Work Unit 11 Flight Date Table	6
Table 5: Lidar specifications and survey settings.....	7
Table 6: Federal Geographic Data Committee monument rating for network accuracy	9
Table 7: Base station positions for the Sierra Nevada acquisition. Coordinates are on the NAD83 (2011) datum, epoch 2010.00	10
Table 8: NV5 ground survey equipment identification.....	11
Table 9: Land Cover Types and Descriptions	12
Table 10: Software used for statistical analysis	15
Table 11: ASPRS LAS classification standards applied to the Sierra Nevada dataset	16
Table 12: Lidar processing workflow	17
Table 13: Work Unit 11 average lidar point densities	21
Table 14: Work Unit 11 absolute accuracy results	25
Table 15: Work Unit 11 vegetated vertical accuracy results	27
Table 16: Work Unit 11 relative accuracy results	29
Table 17: Work Unit 11 Horizontal Accuracy.....	30

INTRODUCTION

This photo, taken by NV5 acquisition staff, shows the high desert mixed landscape in the Sierra Nevada site in California.



In December 2021, NV5 was contracted by The University of California San Diego and the United States Geological Survey (UCSD & USGS) to collect Light Detection and Ranging (lidar) data in 2021 - 2023 for the Sierra Nevada site in California. Data were collected to aid UCSD & USGS in assessing the topographic and geophysical properties of the study area to support fire mitigation and natural disaster mitigation mapping.

This report accompanies the delivered lidar data for the Work Unit 11 area of interest, and documents contract specifications, data acquisition procedures, processing methods, and analysis of the final dataset including lidar accuracy and density. Acquisition dates and acreage are shown in Table 1, deliverable projection information is shown in Table 2, a complete list of contracted deliverables provided to UCSD & USGS is shown in Table 3, and the project extent is shown in Figure 1.

Table 1: Acquisition dates, acreage, and data types collected on the Sierra Nevada site

Project Site	Contracted Square Miles	Buffered Square Miles	Work Unit 11 Square Miles	Acquisition Dates	Data Type
Sierra Nevada, California Work Unit 11	30,119	30,204	1,771	6/2/2022, 6/3/2022, 6/4/2022, 6/6/2022, 6/7/2022, 6/8/2022, 6/9/2022, 6/10/2022, 6/11/2022, 6/14/2022, 6/15/2022, 7/9/2022, 7/10/2022, 8/25/2022, 8/26/2022	NIR - Lidar

Deliverable Products

Table 2: Deliverable product projection information

Projections	Horizontal Datum	Vertical Datum	Units
UTM Zone 11 North	NAD83 (2011)	NAV88 (GEOID18) GRS 1980	Meters

Table 3: Products delivered to UCSD & USGS for the Sierra Nevada Work Unit 11 site

Product Type	File Type	Product Details
Points	LAS v.1.4 (*.las)	<ul style="list-style-type: none"> All Classified Returns
Rasters	0.5 meter GeoTiffs (*.tif)	<ul style="list-style-type: none"> Hydroflattened Bare Earth Digital Elevation Model (DEM) Intensity Images
Rasters	1.0 meter GeoTiffs (*.tif)	<ul style="list-style-type: none"> Maximum Surface Height Rasters (MSHR) Swath Separation Rasters
Vectors	Shapefiles (*.shp)	<ul style="list-style-type: none"> Full Project Boundary projected in UTM 11 UTM 11 Data Extent UTM 11 Lidar Tile Index Work Unit 11 Boundary Work Unit 11 Lidar Tile Index
Vectors	ESRI File Geodatabase (*.gdb)	<ul style="list-style-type: none"> 3D Waters Edge Breaklines 3D Bridge Breaklines Flightline Index Flightline Swaths
Metadata	Extensible Markup Language (*.xml)	<ul style="list-style-type: none"> Metadata
Reports	Adobe Acrobat (*.pdf)	<ul style="list-style-type: none"> Lidar Technical Data Report Calibration folder

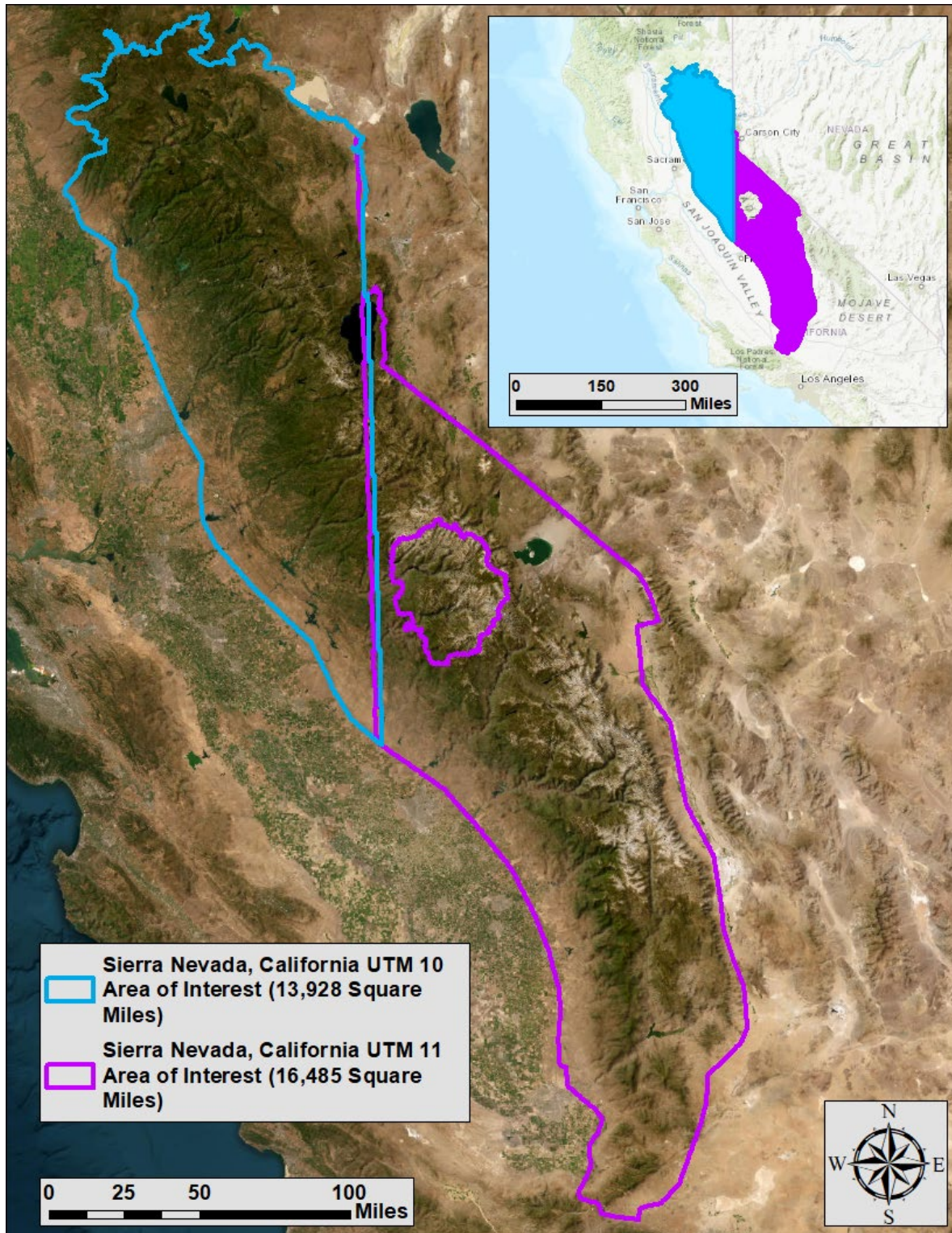


Figure 1: Location map of the Sierra Nevada site in California

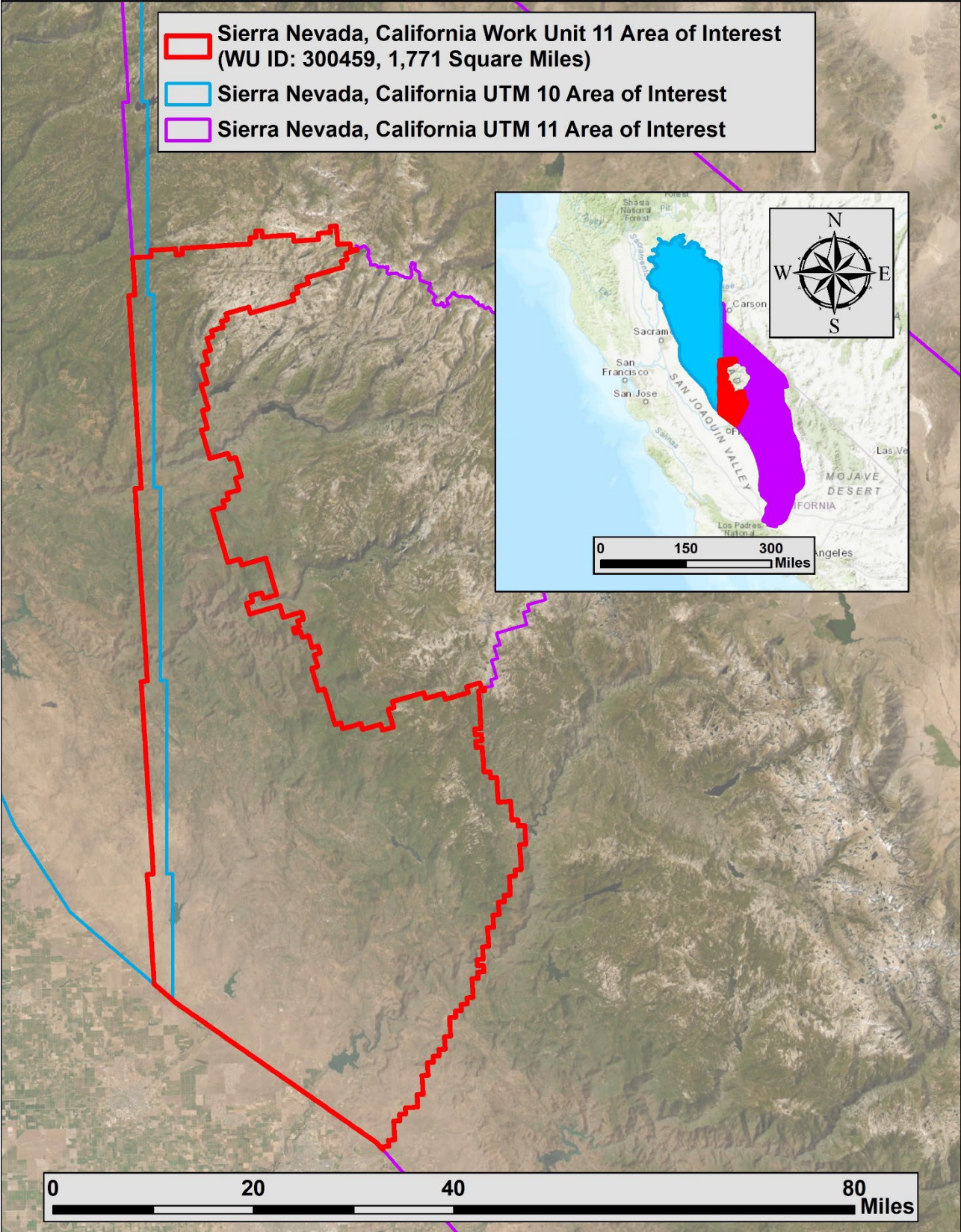


Figure 2: Location map of the Sierra Nevada Work Unit 11 site in California

ACQUISITION

NV5's ground acquisition equipment set up in the Sierra Nevada Lidar study area.



Planning

In preparation for data collection, NV5 reviewed the project area and developed a specialized flight plan to ensure complete coverage of the Sierra Nevada lidar study area at the QL1 target point density of ≥ 8.0 points/m² (0.74 points/ft²). Acquisition parameters including orientation relative to terrain, flight altitude, pulse rate, scan angle, and ground speed were adapted to optimize flight paths and flight times while meeting all contract specifications. Figure 3 shows these optimized flight paths and dates.

Factors such as satellite constellation availability and weather windows must be considered during the planning stage. Any weather hazards or conditions affecting the flight were continuously monitored due to their potential impact on the daily success of airborne and ground operations. In addition, logistical considerations including private property access and potential air space restrictions were reviewed.

Table 4: Work Unit 11 Flight Date Table

Date	Flight Line Number	Start Time (Adjusted GPS)	End Time (Adjusted GPS)
6/2/2022	7405 – 7420	338200343	338214667
6/3/2022	13510 – 13525	338289807	338300963
6/4/2022	14000 – 14006, 14300 -14302	338368532	338390494
6/6/2022	10900 – 10919, 13935 – 13945	338542003	338560284
6/7/2022	12300 – 12305, 12700 – 12716	338627897	338646630
6/8/2022	11136 – 11143, 12100 – 12134	338714437	338730541
6/9/2022	11400 – 11414, 11416 – 11422, 12401 – 12418	338805203	338823449
6/10/2022	12500 – 12502, 12504 - 12517, 13000 – 13002	338888649	338905177
6/11/2022	11500 – 11519, 11521 – 11529, 11601 - 11620	338970850	339007853
6/14/2022	13100 – 13124	339239713	339252386
6/15/2022	10407 – 10416	339324413	339330227
7/9/2022	6827 – 6831, 6833 – 6834, 6836	341407147	341409906
7/10/2022	6731, 10503, 10505 – 10521	341480227	341495148
8/25/2022	7602 – 7619	345454499	345460065
8/26/2022	7734 – 7743	345553347	345557771

Airborne Lidar Survey

The lidar survey was accomplished using a Riegl VQ-1560ii-S system mounted in a Cessna Caravan. Table 5 summarizes the settings used to yield an average pulse density of ≥ 8 pulses/m² over the Sierra Nevada project area. The Riegl VQ-1560ii-S laser system can record unlimited range measurements (returns) per pulse, however a maximum of 15 returns can be stored due to LAS v1.4 file limitations. The typical number of returns digitized from a single pulse range from 1 to 14 for the Sierra Nevada project area. It is not uncommon for some types of surfaces (e.g., dense vegetation or water) to return fewer pulses to the lidar sensor than the laser originally emitted. The discrepancy between first return and overall delivered density will vary depending on terrain, land cover, and the prevalence of water bodies. All discernible laser returns were processed for the output dataset. Figure 3 shows the flightlines acquired using these lidar specifications.

Table 5: Lidar specifications and survey settings

Parameter	NIR Laser
Acquisition Dates	6/2/2022 – 8/26/2022
Aircraft Used	Cessna Caravan
Sensor	Riegl
Laser	VQ-1560ii-S
Maximum Returns	14
Resolution/Density	Average 8 pulses/m ²
Nominal Pulse Spacing	0.35 m
Survey Altitude (AGL)	2,500 m
Survey speed	145 knots
Field of View	58.5°
Mirror Scan Rate	Uniform Point Spacing
Target Pulse Rate	757 kHz
Pulse Length	3.0 ns
Scanner Pulse Width	90 cm
Central Wavelength	1064 nm
Pulse Mode	Multiple Times Around (MTA)
Beam Divergence	0.23 mrad
Swath Width	2,800 m
Swath Overlap	50%
Intensity	16-bit
Vertical Accuracy	RMSE _z (Non-Vegetated) \leq 10 cm
NVA Accuracy	NVA (95% Confidence Level) \leq 19.6 cm
VVA Accuracy	VVA (95 th Percentile) \leq 30 cm



Riegl VQ-1560ii-S

All areas were planned for an opposing flight line side-lap of $\geq 50\%$ ($\geq 100\%$ overlap) to reduce laser shadowing and increase surface laser painting. In some areas of steep elevation change 50% overlap was not achieved, nonetheless, these areas meet the QL1 project density. To accurately solve for laser point position (geographic coordinates x, y, and z), the positional coordinates of the airborne sensor and the orientation of the aircraft to the horizon (attitude) were recorded continuously throughout the lidar data collection mission. Position of the aircraft was measured twice per second (2 Hz) by an onboard differential GPS unit, and aircraft attitude was measured 200 times per second (200 Hz) as pitch, roll and yaw (heading) from an onboard inertial measurement unit (IMU). To allow for post-processing correction and calibration, aircraft and sensor position and attitude data are indexed by GPS time.

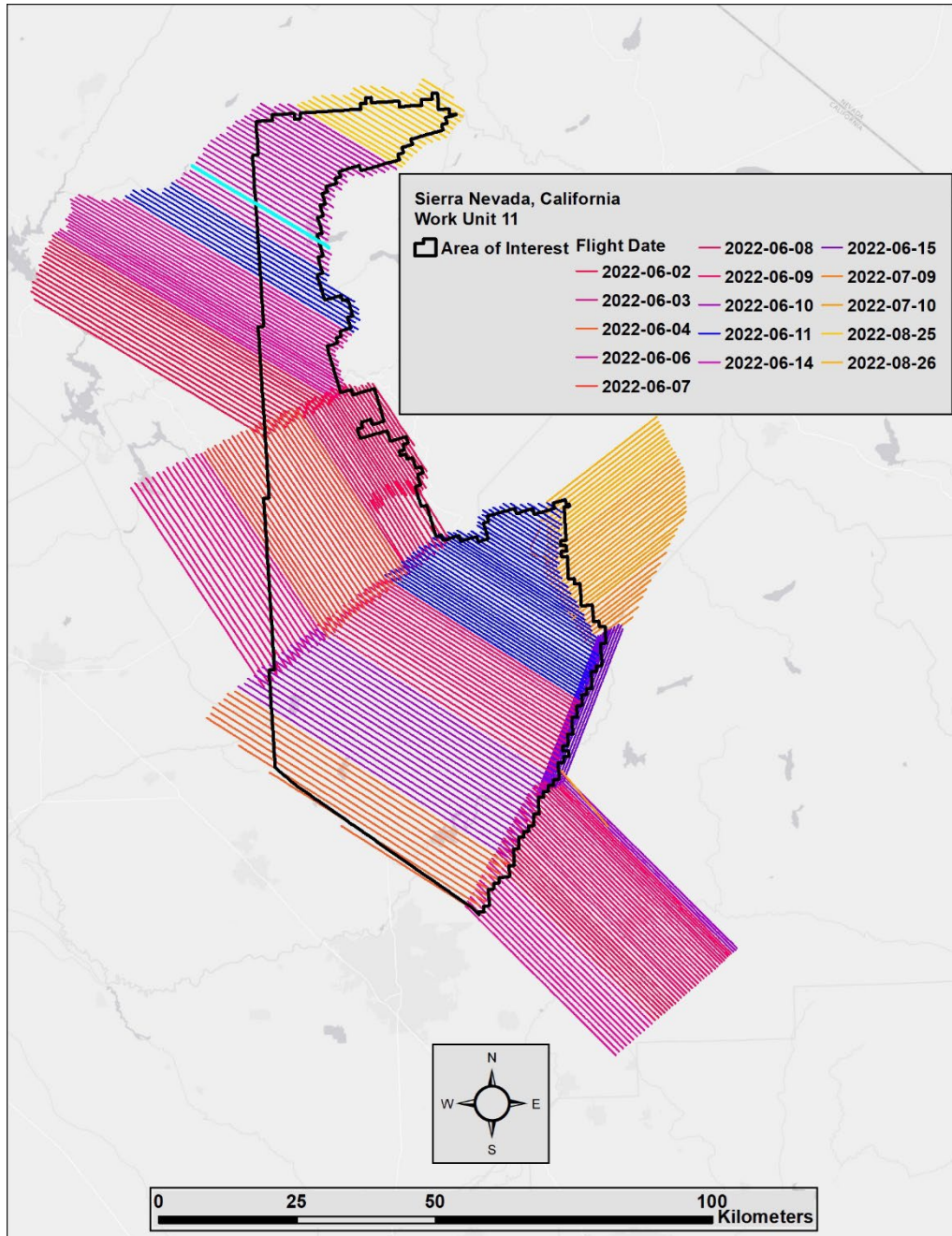


Figure 3: Work Unit 11 flightlines map

Ground Survey

Ground control surveys, including monumentation, and ground survey points (GSPs) were conducted to support the airborne acquisition. Ground control data were used to geospatially correct the aircraft positional coordinate data and to perform quality assurance checks on final lidar products.

Base Stations

Base stations were utilized for collection of ground survey points using real time kinematic (RTK), fast static (FS), and total station (TS) survey techniques (Table 7, Figure 4).

Base station locations were selected with consideration for satellite visibility, field crew safety, and optimal location for GSP coverage. NV5 utilized 16 permanent real-time network (RTN) base stations from the Hexagon SmartNet and California Surveying and Drafting Supply (CSDS) networks, 14 new and existing monuments, and one NGS base station for the Sierra Nevada Lidar project. NV5 established 12 new monuments using 6" mag hub nails with orange survey washers and utilized two existing California Spatial Reference Center (CSRC) monuments. NV5's professional land surveyor Evon Silvia (CAPLS#9401) oversaw and certified the ground survey.

NV5 utilized static Global Navigation Satellite System (GNSS) data collected at 1 Hz recording frequency for each base station. During post-processing, the static GNSS data were triangulated with nearby Continuously Operating Reference Stations (CORS) using the Online Positioning User Service (OPUS¹) for precise positioning. Multiple independent sessions over the same monument were processed to confirm antenna height measurements and to refine position accuracy.

Monuments were established according to the national standard for geodetic control networks, as specified in the Federal Geographic Data Committee (FGDC) Geospatial Positioning Accuracy Standards for geodetic networks.² This standard provides guidelines for classification of monument quality at the 95% confidence interval as a basis for comparing the quality of one control network to another. The monument rating for this project is shown in Table 6.

Table 6: Federal Geographic Data Committee monument rating for network accuracy

Direction	Rating
1.96 * St Dev _{NE} :	0.020 m
1.96 * St Dev _z :	0.050 m

¹ OPUS is a free service provided by the National Geodetic Survey to process corrected monument positions. <http://www.ngs.noaa.gov/OPUS>.

² Federal Geographic Data Committee, Geospatial Positioning Accuracy Standards (FGDC-STD-007.2-1998). Part 2: Standards for Geodetic Networks, Table 2.1, page 2-3: [FGDC Standards Website](#)

For the Sierra Nevada Lidar project, the monument coordinates contributed no more than 5.6 cm of positional error to the geolocation of the final ground survey points and lidar, with 95% confidence.

Table 7: Base station positions for the Sierra Nevada acquisition.
Coordinates are on the NAD83 (2011) datum, epoch 2010.00

Base ID	Latitude	Longitude	Ellipsoid (meters)	Owner/Type
89PLU	40° 06' 31.21167"	-120° 54' 27.16654"	1054.746	CSRC / Monument
CACH	39° 42' 50.90381"	-121° 48' 18.99053"	43.933	SMARTNET / RTN
CACR	40° 18' 34.61612"	-121° 13' 44.72082"	1365.022	SMARTNET / RTN
CAEG	38° 22' 51.96521"	-121° 21' 54.25715"	-9.318	SMARTNET / RTN
CAOD	37° 46' 09.98122"	-120° 50' 16.01202"	21.510	SMARTNET / RTN
CAOV	39° 29' 46.71485"	-121° 36' 35.12665"	38.645	SMARTNET / RTN
CAPV	38° 41' 50.41539"	-120° 49' 27.00363"	530.245	SMARTNET / RTN
CARK	38° 47' 25.35750"	-121° 18' 45.30085"	18.867	SMARTNET / RTN
CASV	40° 22' 44.64976"	-120° 27' 55.97377"	1232.01	SMARTNET / RTN
CH1F	39° 45' 41.22825"	-121° 52' 00.85247"	34.785	SMARTNET / RTN
CLAPPE	40° 00' 32.98259"	-121° 11' 27.36742"	762.831	CSRC / Monument
GV1K	39° 13' 58.76859"	-121° 02' 34.75684"	794.139	CSDS / RTN
LD1J	38° 08' 13.57317"	-121° 15' 14.58255"	-6.810	CSDS / RTN
MD1I	37° 38' 55.34920"	-120° 58' 39.86345"	6.466	CSDS / RTN
OR1J	39° 30' 18.80455"	-121° 33' 09.27255"	40.770	CSDS / RTN
P147	39° 56' 14.57671"	-120° 17' 03.83554"	2489.452	SMARTNET / RTN
SACR	38° 39' 17.97072"	-121° 21' 15.19293"	7.472	NGS / CORS
SS1H	38° 39' 58.90613"	-120° 56' 14.91233"	457.080	CSDS / RTN
UCSD_FIRE_01	39° 56' 56.34188"	-121° 03' 08.06376"	1091.912	NV5 / Monument
UCSD_FIRE_02	39° 56' 53.63000"	-120° 55' 28.47964"	1015.157	NV5 / Monument
UCSD_FIRE_03	39° 03' 22.38766"	-121° 19' 19.98511"	69.955	NV5 / Monument
UCSD_FIRE_04	39° 27' 12.43661"	-121° 16' 55.40021"	601.255	NV5 / Monument
UCSD_FIRE_05	39° 05' 19.17748"	-120° 57' 15.16457"	663.274	NV5 / Monument
UCSD_FIRE_07	38° 50' 30.36441"	-120° 53' 19.21374"	562.810	NV5 / Monument
UCSD_FIRE_08	38° 26' 08.11181"	-120° 33' 04.97841"	933.475	NV5 / Monument
UCSD_FIRE_09	40° 10' 51.54205"	-120° 36' 28.94102"	1509.712	NV5 / Monument
UCSD_FIRE_10	40° 03' 19.84580"	-121° 35' 39.71582"	1357.788	NV5 / Monument
UCSD_FIRE_11	39° 58' 59.31845"	-121° 16' 55.60642"	633.738	NV5 / Monument
UCSD_FIRE_12	39° 53' 59.64192"	-121° 31' 11.52379"	1050.214	NV5 / Monument

Base ID	Latitude	Longitude	Ellipsoid (meters)	Owner/Type
UCSD_FIRE_13	39° 35' 09.29564"	-121° 04' 40.80538"	1192.909	NV5 / Monument
YC1H	39° 08' 43.40979"	-121° 38' 33.44751"	-3.477	CSDS / RTN

Ground Survey Points (GSPs)

Ground survey points were collected using real time kinematic (RTK), fast-static (FS), and total station (TS) survey techniques. For RTK surveys, a roving receiver receives corrections from a nearby base station or Real-Time Network (RTN) via radio or cellular network, enabling rapid collection of points with relative errors less than 1.5 cm horizontal and 2.0 cm vertical. FS surveys compute these corrections during post-processing to achieve comparable accuracy. RTK surveys record data while stationary for at least five seconds, calculating the position using at least three one-second epochs. FS surveys record observations for up to fifteen minutes on each GSP to support longer baselines. All GSP measurements were made during periods with a Position Dilution of Precision (PDOP) of ≤ 3.0 with at least six satellites in view of the stationary and roving receivers. See Table 8 for Trimble unit specifications.

Forested checkpoints are collected using total stations to measure positions under dense canopy. Total station backsight and setup points are established using GNSS survey techniques.

GSPs were collected in areas where good satellite visibility was achieved on paved roads and other hard surfaces such as gravel or packed dirt roads. GSP measurements were not taken on highly reflective surfaces such as center line stripes or lane markings on roads due to the increased noise seen in the laser returns over these surfaces. GSPs were collected within as many flightlines as possible; however, the distribution of GSPs depended on ground access constraints and monument locations and may not be equably distributed throughout the study area (Figure 4).

Table 8: NV5 ground survey equipment identification

Receiver Model	Antenna	OPUS Antenna ID	Use
Trimble R8 Model 3	Integrated Antenna	TRMR8_GNSS3	Rover
Trimble R10 Model 2	Integrated Antenna	TRMR10-2	Rover and Static
Trimble R12	Integrated Antenna	TRMR12	Rover
Nikon NPL-322+ 5" P Total Station	N/A	n/a	VVA
Trimble M3 Total Station	N/A	n/a	VVA

Land Cover Class

In addition to ground survey points, land cover class checkpoints were collected throughout the study area to evaluate vertical accuracy. Vertical accuracy statistics were calculated for all land cover types to assess confidence in the lidar derived ground models across land cover classes (Table 9, see Lidar Accuracy Assessments, page 24).

Table 9: Land Cover Types and Descriptions

Land Cover Type	Land Cover Code	Example	Description	Accuracy Assessment Type
Shrub	SH		Low growth shrub	VVA
Tall Grass	TG		Herbaceous grasslands in advanced stages of growth	VVA
Forest	FR		Forested areas	VVA
Bare Earth	BE		Areas of bare earth surface	NVA
Urban	UA		Areas dominated by urban development, including parks	NVA

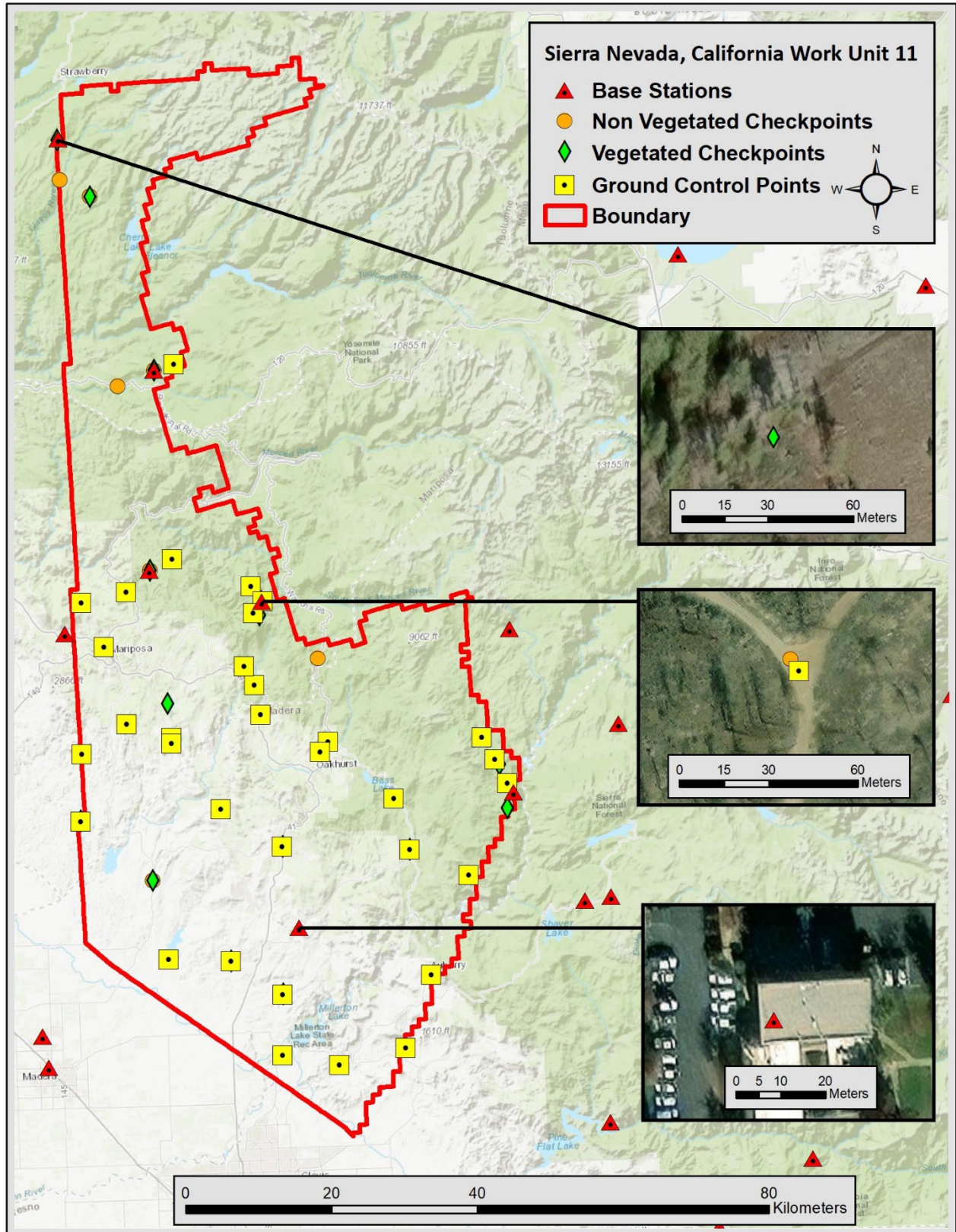


Figure 4: Work Unit 11 ground survey location map

PROCESSING



This view shows the Stanislaus National Forest within the Work Unit 11 area of interest. The image was created from the lidar point cloud colored by intensity.

Boresight Calibration

Prior to the lidar acquisition, NV5 collects sample lidar data in support of sensor calibration and geometric adjustments for all sensor and aircraft combinations utilized in the airborne acquisition. These data support boresight analysis to properly position the sensor orientation within the aircraft. This process, performed in Applanix PosPac, is essential for data interswath adjustments performed during the calibration phase. Additional details on geometric adjustments can be found in Appendix A - Accuracy Controls.

GNSS-Inertial Processing

Applanix + POSpac software was used for post-processing of airborne GPS and inertial data (IMU), which is critical to the positioning and orientation of the lidar sensor during all flights. Applanix POSpac combines aircraft raw trajectory data with stationary GPS base station data yielding a “Smoothed Best Estimate Trajectory” (SBET) necessary for additional post processing software to develop the resulting geo-referenced point cloud from the lidar missions (Table 12). SBET quality reports for each processing group have been provided in the file “SBET_QC_Reports.zip” that accompanies this report.

During the sensor trajectory processing (combining GPS & IMU datasets) certain statistical graphs and tables are generated within the Applanix POSpac processing environment which are commonly used as indicators of processing stability and accuracy. This data for analysis includes max horizontal and vertical GPS variance, separation plot, altitude plot, PDOP plot, base station baseline length, processing mode, number of satellite vehicles, and mission trajectory.

Deliverables Processing

Point clouds were created using RiPROCESS software. The generated point cloud is the mathematical three-dimensional composite of all returns from all laser pulse returns from the aerial data collection. The point cloud is processed with GeoCue distributive processing software integrated with Terrasolid software. Imported data is tiled and then calibrated using TerraMatch and NV5 proprietary software. Using TerraScan, the vertical accuracy of the surveyed ground control is tested and any bias is removed from the data. TerraScan and TerraModeler software packages are then used for automated data classification (Table 11) and manual cleanup. Outliers, geometrically unreliable points near the extreme edge of the swath, and any other points deemed unusable are identified using the withheld bit flag. Withheld classes are identified by an Extra Byte in the LAS file set to 1 to indicate that the point should be omitted from further modeling. The data are manually reviewed, and any remaining artifacts removed using functionality provided by TerraScan and TerraModeler.

DEMs and Intensity Images are then generated using NV5 proprietary software. In the bare earth surface model, above-ground features are excluded from the data set. ESRI ArcMap and Global Mapper are used as a final check of the bare earth dataset. Finally, NV5 proprietary software is used to perform statistical analysis of the LAS files (Table 14).

Table 10: Software used for statistical analysis

Statistical Software	Version
Applanix + POSPac	8.7
LASMonkey	2.6.7
RiPROCESS	1.8.6
GeoCue	2020.1.22.1
ESRI Arc Map	10.8
TerraModeler	21.008
TerraScan	21.016

Table 11: ASPRS LAS classification standards applied to the Sierra Nevada dataset

Classification Number	Classification Name	Point Count	Classification Description
1	Default/Unclassified	83,150,950,315	Laser returns that are not included in the ground class, composed of vegetation and anthropogenic features
1W	Edge Clip/Withheld	4,919,669,621	Laser returns at the outer edges of flightlines that are geometrically unreliable
2	Ground	27,701,913,738	Laser returns that are determined to be ground using automated and manual cleaning algorithms
7W	Low Noise/Withheld	213,729,817	Laser returns that are often associated with artificial points below the ground surface
9	Water	130,060,823	Laser returns that are determined to be water using automated and manual cleaning algorithms
17	Bridge	707,159	Bridge decks
18W	High Noise/Withheld	62,251,602	Laser returns that are often associated with birds or scattering from reflective surfaces.
20	Ignored Ground	1,530,241	Ground points proximate to water's edge breaklines; ignored for correct model creation
22	Temporal Exclusion	8,703,527	Laser returns that are determined to be due to temporal differences in flightlines and are excluded from model creation.

Table 12: Lidar processing workflow

Lidar Processing Step	Software Used
Resolve kinematic corrections for aircraft position data using kinematic aircraft GPS and static ground GPS data. Develop a smoothed best estimate of trajectory (SBET) file that blends post-processed aircraft position with sensor head position and attitude recorded throughout the survey.	POSPac MMS v.8.7
Calculate laser point position by associating SBET position to each laser point return time, scan angle, intensity, etc. Create raw laser point cloud data for the entire survey in *.las (ASPRS v. 1.4) format. Convert data to orthometric elevations by applying a geoid correction.	RiUnite v.1.0.3
Import raw laser points into manageable blocks to perform manual relative accuracy calibration and filter erroneous points. Classify ground points for individual flight lines.	TerraScan v.19.005
Using ground classified points per each flight line, test the relative accuracy. Perform automated line-to-line calibrations for system attitude parameters (pitch, roll, heading), mirror flex (scale) and GPS/IMU drift. Calculate calibrations on ground classified points from paired flight lines and apply results to all points in a flight line. Use every flight line for relative accuracy calibration.	StripAlign v.2.21
Classify resulting data to ground and other client designated ASPRS classifications (Table 11). Assess statistical absolute accuracy via direct comparisons of ground classified points to ground control survey data.	TerraScan v.19.005 TerraModeler v.19.003
Generate bare earth models as triangulated surfaces. Export all surface models as Cloud Optimized GeoTIFFs at a 0.5 meter pixel resolution.	LAS Product Creator 3.0 (NV5 proprietary) ArcMap v. 10.8
Generate maximum surface height rasters as a surface expression of all classified points. Generate swath separation images using a grid based average algorithm. Export all surface models as Cloud Optimized GeoTIFFs at a 1.0 meter pixel resolution.	LAS Product Creator 3.0 (NV5 proprietary) ArcMap v. 10.8
Correct intensity values for variability and export intensity images as Cloud Optimized GeoTIFFs at a 0.5 meter pixel resolution.	LAS Product Creator 3.0 (NV5 proprietary) ArcMap v. 10.8

Feature Extraction

Hydroflattening and Water's Edge Breaklines

Millerton Lake, eastern sections of the Merced and Tuolumne Rivers, Cherry Lake, Bass Lake, and other water bodies within the project area were flattened to a consistent water level. Bodies of water that were flattened include lakes and other closed water bodies with a surface area greater than 2 acres, all streams and rivers that are nominally wider than 30 meters, all non-tidal waters bordering the project, and select smaller bodies of water as feasible. The hydroflattening process eliminates artifacts in the digital terrain model caused by both increased variability in ranges and dropouts in laser returns due to the low reflectivity of water.

Hydroflattening of closed water bodies was performed through a combination of automated and manual detection and adjustment techniques designed to identify water boundaries and water levels. Boundary polygons were developed using an algorithm which weights lidar-derived slopes, intensities, and return densities to detect the water's edge. The water edges were then manually reviewed and edited as necessary. Specific care was taken to not hydroflatten wetland and marsh habitat found throughout the study site.

Once polygons were developed the initial ground classified points falling within water polygons were reclassified as water points to omit them from the final ground model. Elevations were then obtained from the filtered lidar returns to create the final breaklines. Lakes were assigned a consistent elevation for an entire polygon while rivers were assigned consistent elevations on opposing banks and smoothed to ensure downstream flow through the entire river channel.

Water boundary breaklines were then incorporated into the hydroflattened DEM by enforcing triangle edges (adjacent to the breakline) to the elevation values of the breakline. This implementation corrected interpolation along the hard edge. Water surfaces were obtained from a TIN of the 3-D water edge breaklines resulting in the final hydroflattened model (Figure 5).

Please note due to the nature of the long flightlines required for the lidar acquisition, there are perceptible temporal differences in water surface elevation within some of the lakes, reservoirs, and other impoundments within the project area. NV5 has elected to express these differences in water surface elevation where apparent so that the hydroflattened bare earth model and corresponding breaklines accurately reflect water surface elevation at the time of acquisition (Figure 6).

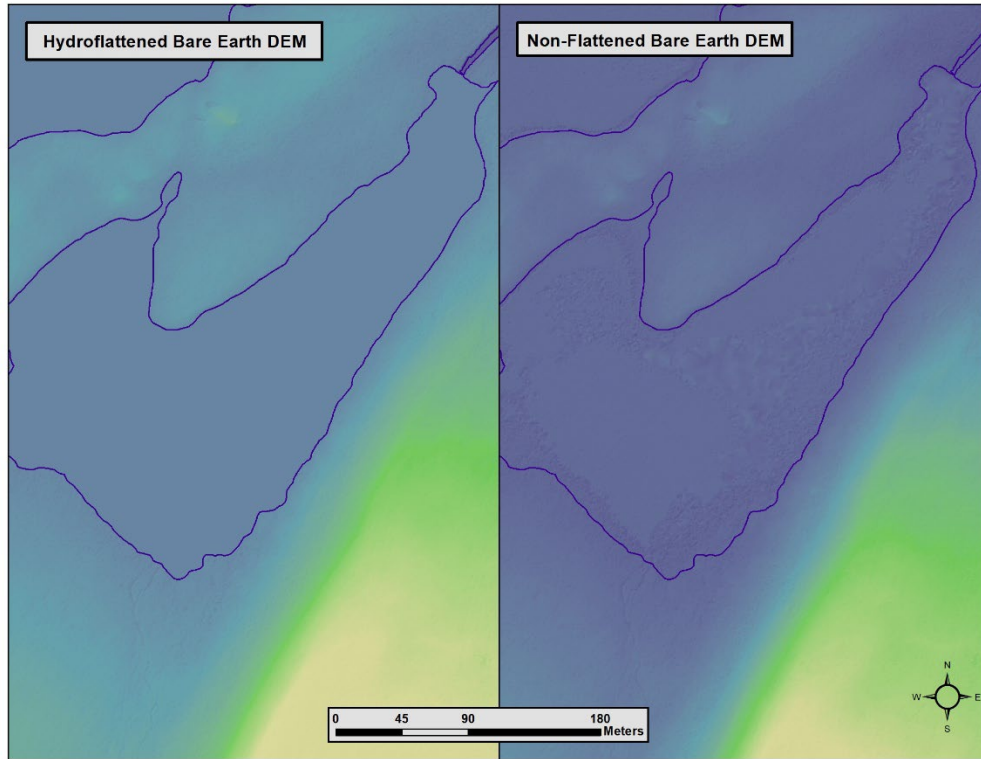


Figure 5: Example of hydroflattening in the Sierra Nevada Lidar dataset

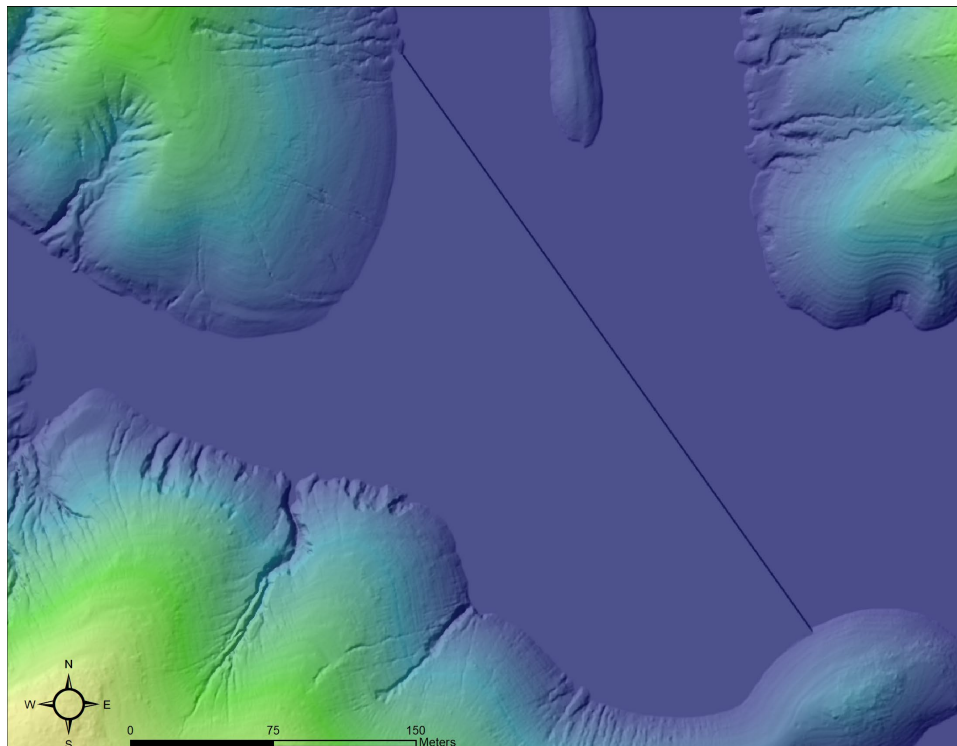


Figure 6: Example of hydroflattening treatment applied to a reservoir with temporal water surface variation within the Sierra Nevada Lidar dataset

Swath Separation Raster Processing

Swath Separation Images are rasters that represent the interswath alignment between flight lines and provide a qualitative evaluation of the positional quality of the point cloud. NV5 proprietary software generated 1-meter raster images in GeoTIFF format using all returns from all the classes (Table 11), excluding points flagged with the withheld bit, and using a grid based average algorithm. Images are generated with 50% intensity opacity and four absolute 8-cm intervals (see Figure 7 below for interval coloring). Intensity images are linearly scaled to a value range specific to the project area and sensor to standardize the images and reduce differences between individual flightlines. Appropriate horizontal projection information as well as applicable header values are written to the file during product generation. NV5 uses a proprietary tool called FOCUS on Delivery to check all formatting requirements of the images against what is required before final delivery.





	0-8cm
	8-16cm
	16-24cm
	>24cm

Figure 7: The color ramp values used in the Sierra Nevada project

This view shows the Stanislaus National Forest within the Work Unit 11 area of interest. The image was created from the lidar point cloud colored by intensity



Lidar Density

The acquisition parameters were designed to acquire an average first-return density of 8 points/m². First return density describes the density of pulses emitted from the laser that return at least one echo to the system. Multiple returns from a single pulse were not considered in the first return density analysis. Some types of surfaces (e.g., breaks in terrain, water and steep slopes) may have returned fewer pulses than originally emitted by the laser. First returns typically reflect off the highest feature on the landscape within the footprint of the pulse. In forested or urban areas, the highest feature could be a tree, building or power line, while in areas of unobstructed ground, the first return will be the only echo and represents the bare earth surface.

The density of ground-classified lidar returns was also analyzed for this project. Terrain character, land cover, and ground surface reflectivity all influenced the density of ground surface returns. In vegetated areas, fewer pulses may penetrate the canopy, resulting in lower ground density.

The average first-return density of lidar data for the Sierra Nevada Work Unit 11 project area was 16.55 points/m² while the average ground classified density was 6.07 points/m² (Table 13). The statistical and spatial distributions of first return densities and classified ground return densities per 100 m x 100 m cell are portrayed in Figure 8 through Figure 10.

Table 13: Work Unit 11 average lidar point densities

Classification	Point Density
First-Return	16.50 points/m ²
Ground Classified	6.07 points/m ²

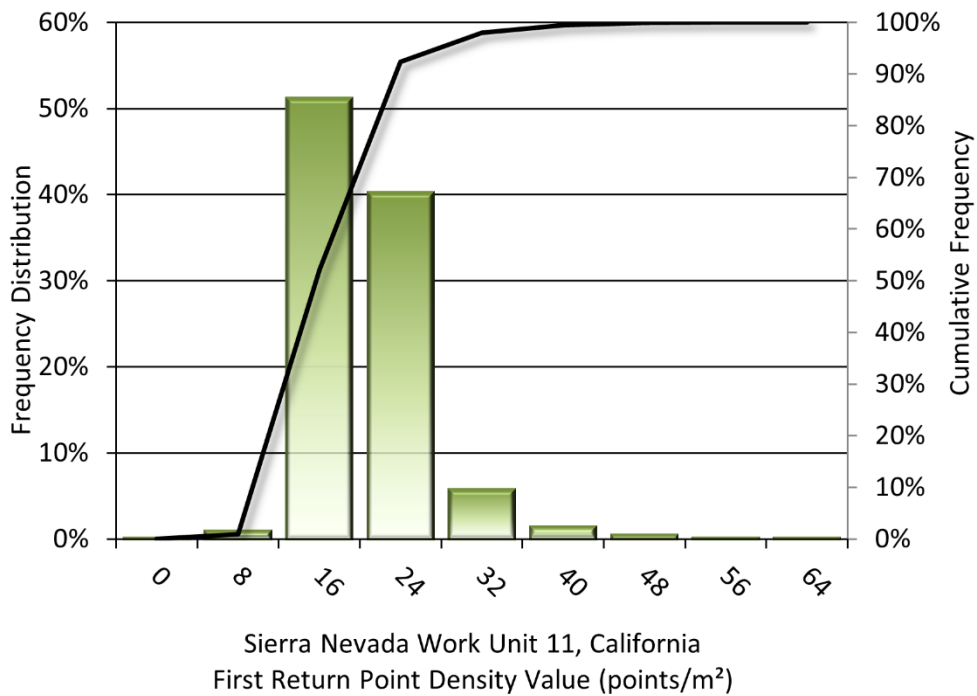


Figure 8: Frequency distribution of first return point density values per 100 x 100 m cell

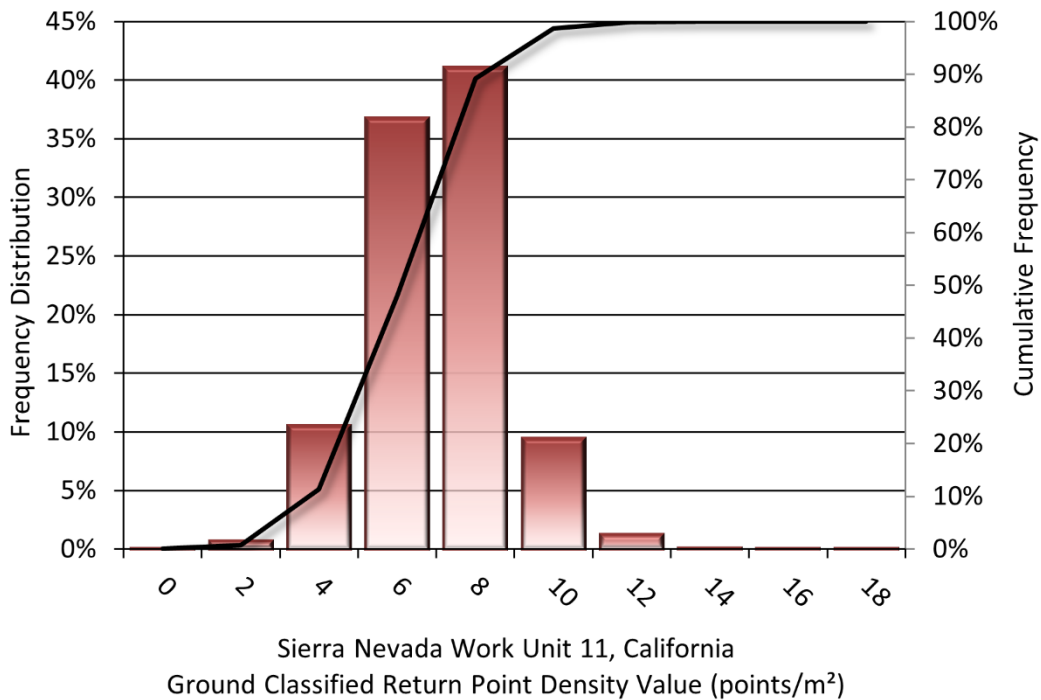


Figure 9: Frequency distribution of ground-classified return point density values per 100 x 100 m cell

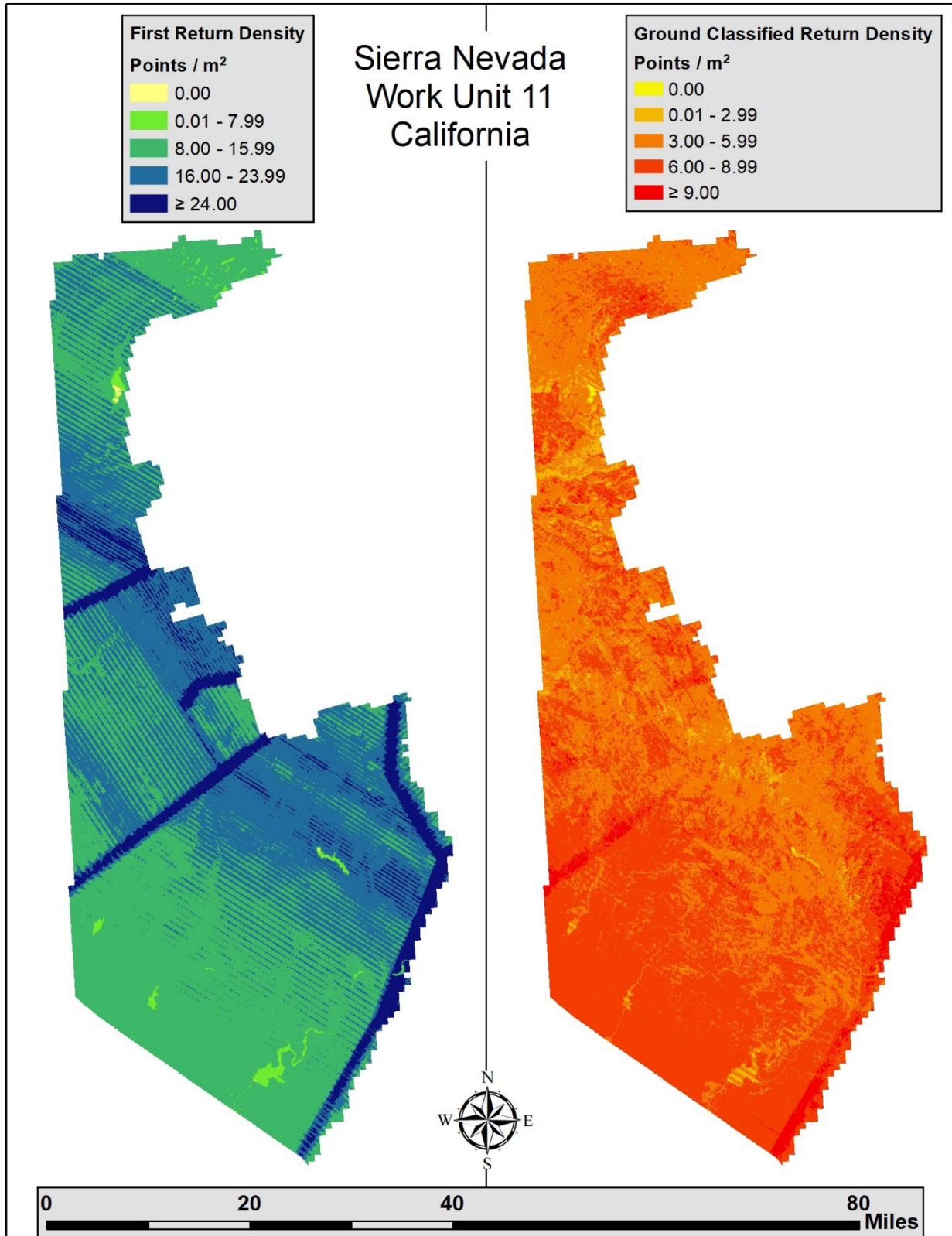


Figure 10: First return and ground point density map for the Sierra Nevada Work Unit 11 site (100 m x 100 m cells)

Lidar Accuracy Assessments

The accuracy of the lidar data collection can be described in terms of absolute accuracy (the consistency of the data with external data sources) and relative accuracy (the consistency of the dataset with itself). See Appendix A - Accuracy Controls for further information on sources of error and operational measures used to improve relative accuracy.

Lidar Non-Vegetated Vertical Accuracy

Absolute accuracy was assessed using Non-Vegetated Vertical Accuracy (NVA) reporting designed to meet guidelines presented in the FGDC National Standard for Spatial Data Accuracy³. NVA compares known ground check point data that were withheld from the calibration and post-processing of the lidar point cloud to the triangulated surface generated by the classified lidar point cloud as well as the derived gridded bare earth DEM. NVA is a measure of the accuracy of lidar point data in open areas where the lidar system has a high probability of measuring the ground surface and is evaluated at the 95% confidence interval ($1.96 * RMSE$), as shown in Table 14.

The mean and standard deviation (sigma σ) of divergence of the ground surface model from quality assurance point coordinates are also considered during accuracy assessment. These statistics assume the error for x, y and z is normally distributed, and therefore the skew and kurtosis of distributions are also considered when evaluating error statistics. For the Sierra Nevada Work Unit 11 survey, 27 ground checkpoints were withheld from the calibration and post processing of the lidar point cloud, with resulting non-vegetated vertical accuracy of 0.063 meters as compared to classified LAS, and 0.071 meters as compared to the bare earth DEM, with 95% confidence (Figure 11, Figure 12).

NV5 also assessed absolute accuracy using 33 ground control points. Although these points were used in the calibration and post-processing of the lidar point cloud, they still provide a good indication of the overall accuracy of the lidar dataset, and therefore have been provided in Table 14 and Figure 13.

[1] Federal Geographic Data Committee, [ASPRS POSITIONAL ACCURACY STANDARDS FOR DIGITAL GEOSPATIAL DATA EDITION 2, Version 1.0, August 2023](#).

Table 14: Work Unit 11 absolute accuracy results

Parameter	NVA, as compared to classified LAS	NVA, as compared to bare earth DEM	Ground Control Points
Sample	27 points	27 points	33 points
95% Confidence (1.96*RMSE)	0.063 m	0.071 m	0.072 m
Average	-0.008 m	-0.010 m	-0.006 m
Median	-0.007 m	-0.013 m	-0.001 m
RMSE	0.032 m	0.036 m	0.037 m
Standard Deviation (1σ)	0.032 m	0.035 m	0.037 m

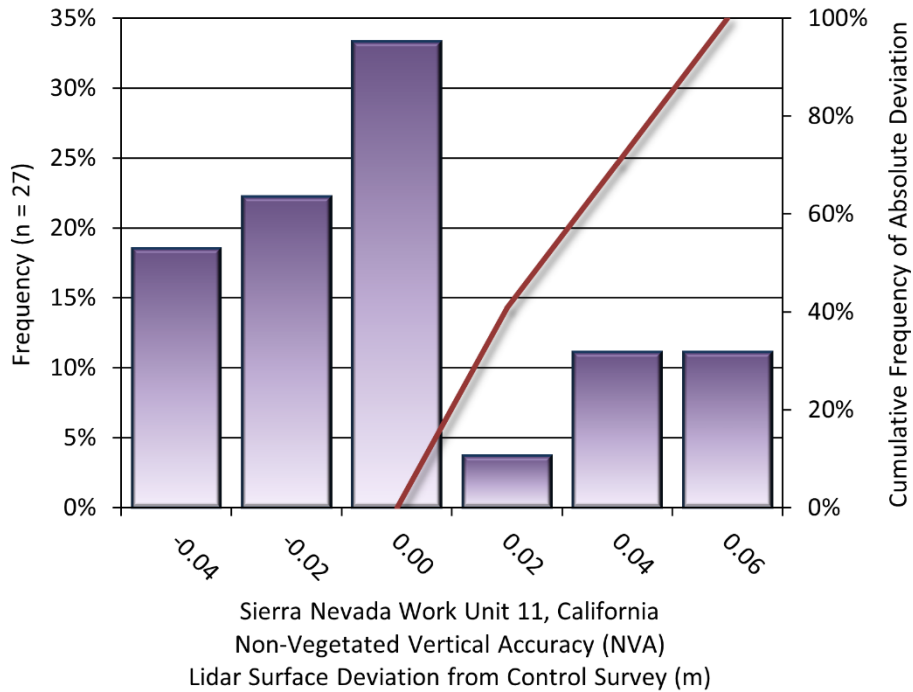


Figure 11: Frequency histogram for lidar classified LAS deviation from ground check point values (NVA)

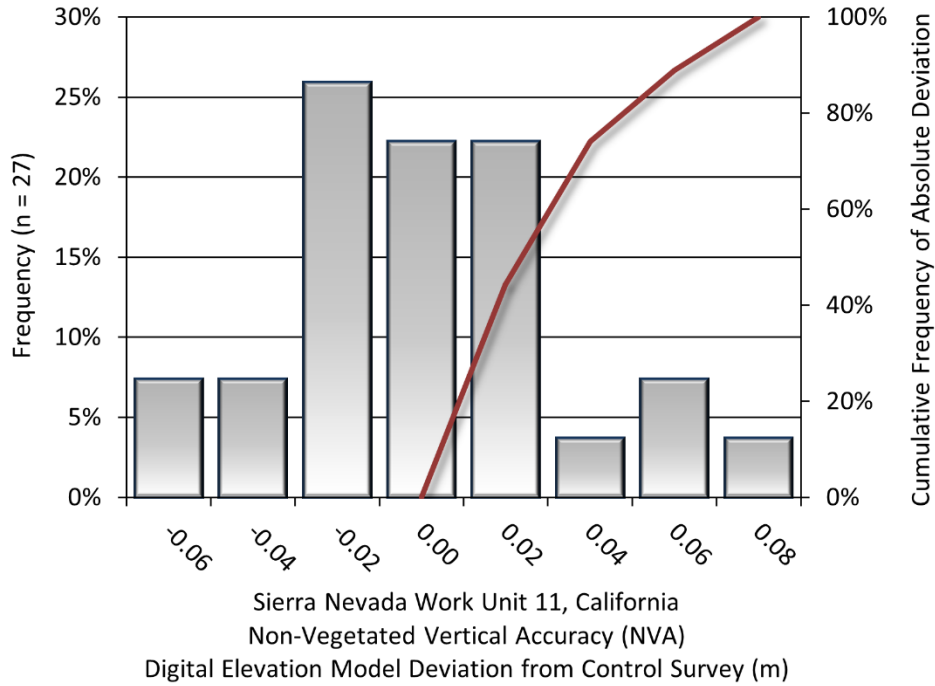


Figure 12: Frequency histogram for the lidar bare earth DEM surface deviation from ground check point values (NVA)

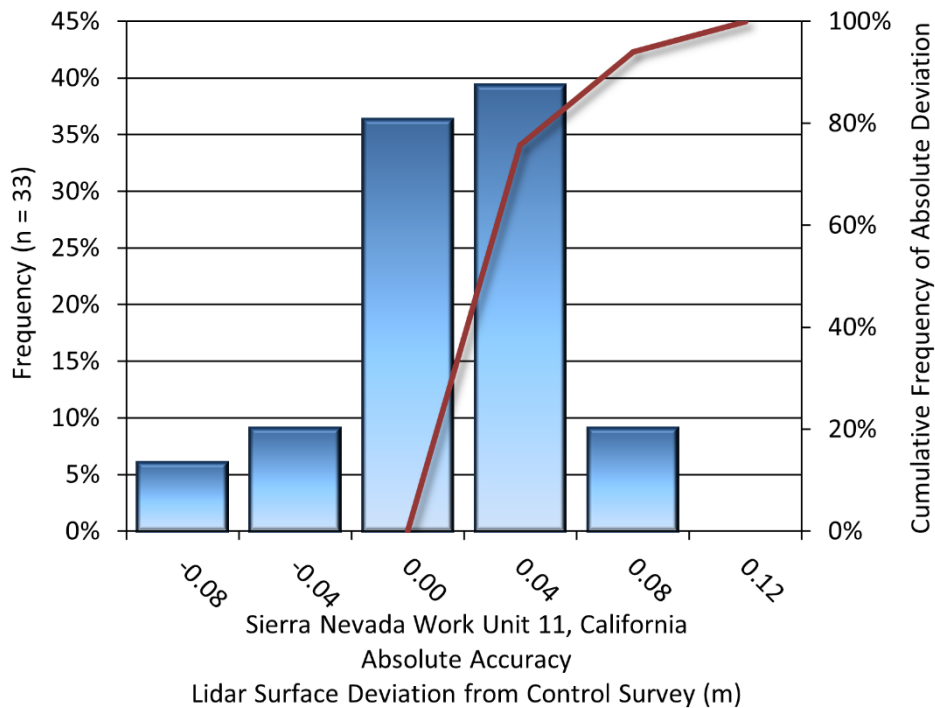


Figure 13: Frequency histogram for the lidar surface deviation from ground control point values

Lidar Vegetated Vertical Accuracies

NV5 also assessed vertical accuracy using Vegetated Vertical Accuracy (VVA) reporting. VVA compares known ground check point data collected over vegetated surfaces using land class descriptions to the triangulated ground surface generated by the ground classified lidar points. For the Sierra Nevada Work Unit 11 survey, 18 vegetated checkpoints were collected, with resulting vegetated vertical accuracy of 0.111 meters as compared to the classified LAS, and 0.135 meters as compared to the bare earth DEM, evaluated at the 95th percentile (Table 15, Figure 14, & Figure 15).

Table 15: Work Unit 11 vegetated vertical accuracy results

Parameter	VVA, as compared to classified LAS	VVA, as compared to bare earth DEM
Sample	18 points	18 points
95 th Percentile	0.111 m	0.135 m
Average	0.026 m	0.036 m
Median	0.014 m	0.027 m
RMSE	0.064 m	0.074 m
Standard Deviation (1 σ)	0.060 m	0.066 m

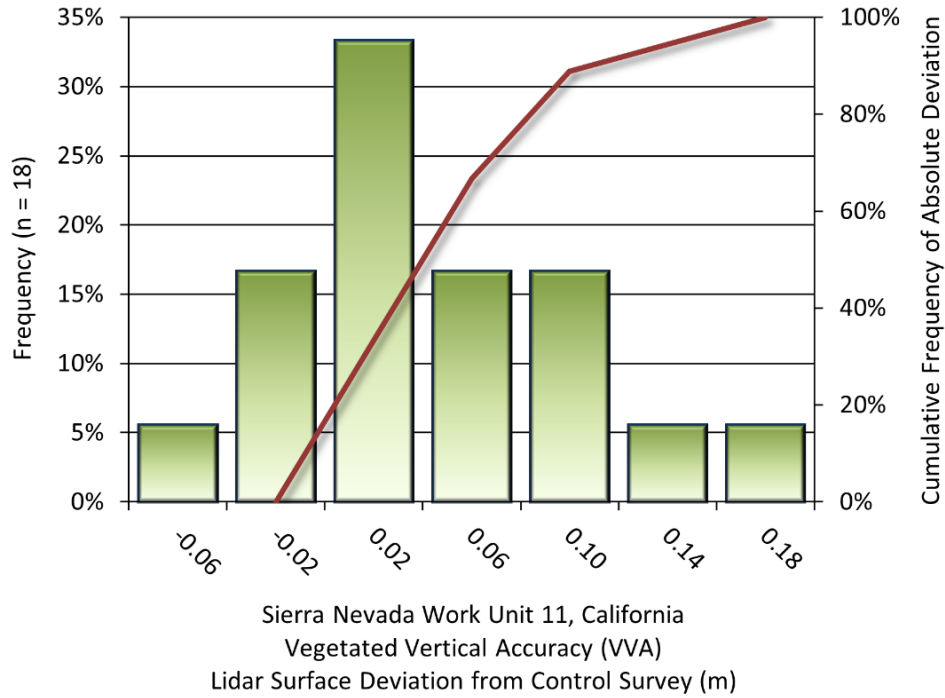


Figure 14: Frequency histogram for the lidar surface deviation from vegetated check point values (VVA)

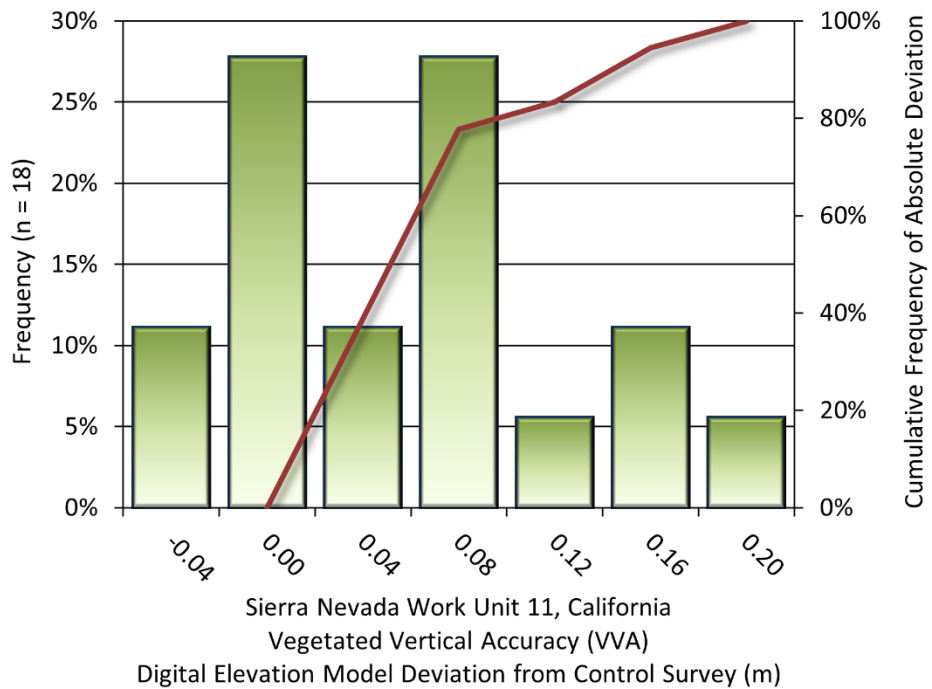


Figure 15: Frequency histogram for the lidar bare earth DEM deviation from vegetated check point values (VVA)

Lidar Relative Vertical Accuracy

Relative vertical accuracy refers to the internal consistency of the data set as a whole: the ability to place an object in the same location given multiple flight lines, GPS conditions, and aircraft attitudes. When the lidar system is well calibrated, the swath-to-swath vertical divergence is low (<0.10 meters). The relative vertical accuracy was computed by comparing the ground surface model of each individual flight line with its neighbors in overlapping regions. The average (mean) line to line relative vertical accuracy for the Sierra Nevada Work Unit 11 Lidar project area was 0.033 meters (Table 16, Figure 16).

Table 16: Work Unit 11 relative accuracy results

Parameter	Relative Accuracy
Sample	338 surfaces
Average	0.033 m
Median	0.035 m
RMSE	0.035 m
Standard Deviation (1σ)	0.007 m
1.96σ	0.014 m

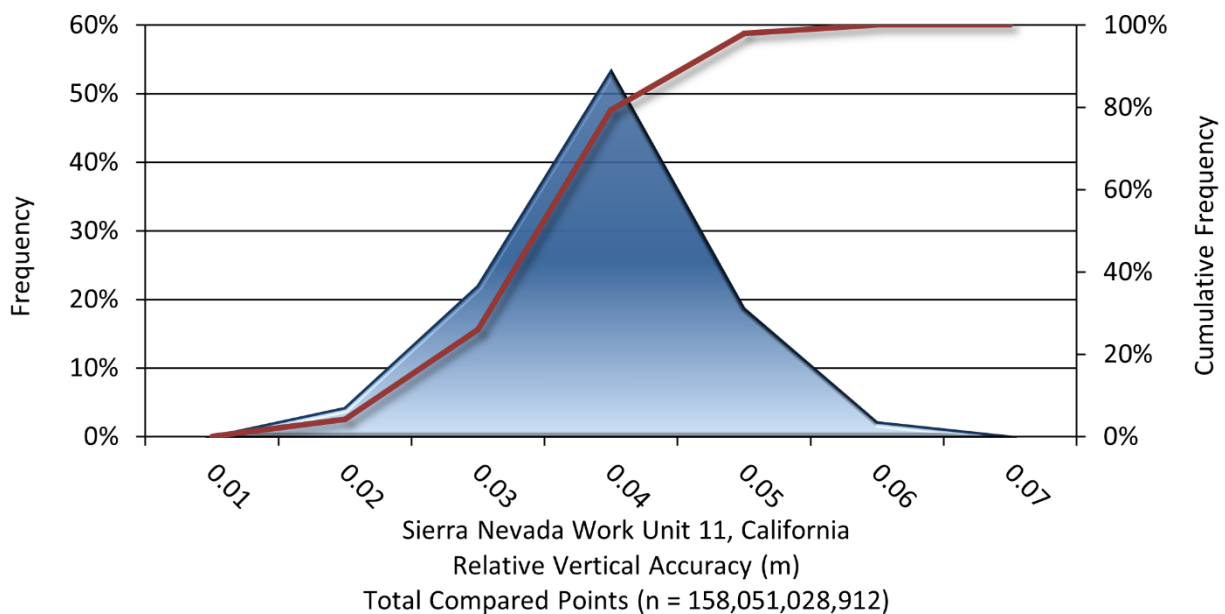


Figure 16: Frequency plot for relative vertical accuracy between flightlines

Intraswath Precision (Smooth Surface Precision)

Intraswath Precision (smooth surface precision) is the measure of reliability of the lidar point cloud elevations along a planar surface. This measurement is performed on hard surfaces against a single flightline. NV5 digitized several large parking lots as polygons across the project area. These polygons were then used to calculate precision on a single flightline basis using the below formula:

$$\text{Precision} = \text{Range} - (\text{Slope} \times \text{Cellsize} \times 1.414)$$

Range – is the difference between the highest and lowest lidar points in each cell

Slope – is the maximum slope of the cell to its 8 neighbors

Cellsize – is set to the ANPS, rounded up to the next integer, and then doubled

NV5 calculated the RMSD_z to be 0.060 meters, minimum slope-corrected range to be 0.020 meters, and the maximum slope-corrected range to be 0.085 meters.

Due to a lack of suitable hard surfaces containing only single return lidar points within the Sierra Nevada project area, intraswath precision could not be calculated for every lift. The intraswath accuracy was calculated only in suitable locations.

Lidar Horizontal Accuracy

Lidar horizontal accuracy is a function of Global Navigation Satellite System (GNSS) derived positional error, flying altitude, and INS derived attitude error. The obtained RMSE_r value is multiplied by a conversion factor of 1.7308 to yield the horizontal component of the National Standards for Spatial Data Accuracy (NSSDA) reporting standard where a theoretical point will fall within the obtained radius 95 percent of the time. Based on a flying altitude of 2,500 meters, an IMU error of 0.002 decimal degrees, and a GNSS positional error of 0.027 meters, this project was produced to meet 0.274 meters horizontal accuracy at the 95% confidence level (Table 17).

Table 17: Work Unit 11 Horizontal Accuracy

Parameter	Horizontal Accuracy
RMSE_r	0.158 m
ACC _r	0.274 m

CERTIFICATIONS

NV5 Geospatial provided lidar services for the Sierra Nevada project as described in this report.

I, John English, have reviewed the attached report for completeness and hereby state that it is a complete and accurate report of this project.

John T. English
John T. English (Jul 31, 2024 14:51 PDT)

Jul 31, 2024

John English
Project Manager
NV5 Geospatial

I, Evon P. Silvia, PLS, being duly registered as a Professional Land Surveyor in and by the state of California, hereby certify that the methodologies, static GNSS occupations used during airborne flights, and ground survey point collection were performed using commonly accepted Standard Practices. Field work conducted for this report was conducted between June 2 and August 26, 2022.

Accuracy statistics shown in the Accuracy Section of this Report have been reviewed by me and found to meet the "National Standard for Spatial Data Accuracy".

Evon P. Silvia Jul 31, 2024

Evon P. Silvia, PLS
NV5 Geospatial
Corvallis, OR 97330



Signed: Jul 31, 2024

GLOSSARY

1-sigma (σ) Absolute Deviation: Value for which the data are within one standard deviation (approximately 68th percentile) of a normally distributed data set.

1.96 * RMSE Absolute Deviation: Value for which the data are within two standard deviations (approximately 95th percentile) of a normally distributed data set, based on the FGDC standards for Non-vegetated Vertical Accuracy (NVA) reporting.

Accuracy: The statistical comparison between known (surveyed) points and laser points. Typically measured as the standard deviation (σ) and root mean square error (RMSE).

Absolute Accuracy: The vertical accuracy of lidar data is described as the mean and standard deviation (σ) of divergence of lidar point coordinates from ground survey point coordinates. To provide a sense of the model predictive power of the dataset, the root mean square error (RMSE) for vertical accuracy is also provided. These statistics assume the error distributions for x, y and z are normally distributed, and thus we also consider the skew and kurtosis of distributions when evaluating error statistics.

Relative Accuracy: Relative accuracy refers to the internal consistency of the data set; i.e., the ability to place a laser point in the same location over multiple flight lines, GPS conditions and aircraft attitudes. Affected by system attitude offsets, scale and GPS/IMU drift, internal consistency is measured as the divergence between points from different flight lines within an overlapping area. Divergence is most apparent when flight lines are opposing. When the lidar system is well calibrated, the line-to-line divergence is low (<10 cm).

Root Mean Square Error (RMSE): A statistic used to approximate the difference between real-world points and the lidar points. It is calculated by squaring all the values, then taking the average of the squares and taking the square root of the average.

Data Density: A common measure of lidar resolution, measured as points per square meter.

Digital Elevation Model (DEM): File or database made from surveyed points, containing elevation points over a contiguous area. Digital terrain models (DTM) and digital surface models (DSM) are types of DEMs. DTMs consist solely of the bare earth surface (ground points), while DSMs include information about all surfaces, including vegetation and man-made structures.

Intensity Values: The peak power ratio of the laser return to the emitted laser, calculated as a function of surface reflectivity.

Nadir: A single point or locus of points on the surface of the earth directly below a sensor as it progresses along its flight line.

Overlap: The area shared between flight lines, typically measured in percent. 100% overlap is essential to ensure complete coverage and reduce laser shadows.

Pulse Rate (PR): The rate at which laser pulses are emitted from the sensor; typically measured in thousands of pulses per second (kHz).

Pulse Returns: For every laser pulse emitted, the number of wave forms (i.e., echoes) reflected back to the sensor. Portions of the wave form that return first are the highest element in multi-tiered surfaces such as vegetation. Portions of the wave form that return last are the lowest element in multi-tiered surfaces.

Real-Time Kinematic (RTK) Survey: A type of surveying conducted with a GPS base station deployed over a known monument with a radio connection to a GPS rover. Both the base station and rover receive differential GPS data and the baseline correction is solved between the two. This type of ground survey is accurate to 1.5 cm or less.

Post-Processed Kinematic (PPK) Survey: GPS surveying is conducted with a GPS rover collecting concurrently with a GPS base station set up over a known monument. Differential corrections and precisions for the GNSS baselines are computed and applied after the fact during processing. This type of ground survey is accurate to 1.5 cm or less.

Scan Angle: The angle from nadir to the edge of the scan, measured in degrees. Laser point accuracy typically decreases as scan angles increase.

Native Lidar Density: The number of pulses emitted by the lidar system, commonly expressed as pulses per square meter.

APPENDIX A - ACCURACY CONTROLS

Relative Accuracy Calibration Methodology:

Manual System Calibration: Calibration procedures for each mission require solving geometric relationships that relate measured swath-to-swath deviations to misalignments of system attitude parameters. Corrected scale, pitch, roll and heading offsets were calculated and applied to resolve misalignments. The raw divergence between lines was computed after the manual calibration was completed and reported for each survey area.

Automated Attitude Calibration: All data were tested and calibrated using TerraMatch automated sampling routines. Ground points were classified for each individual flight line and used for line-to-line testing. System misalignment offsets (pitch, roll and heading) and scale were solved for each individual mission and applied to respective mission datasets. The data from each mission were then blended when imported together to form the entire area of interest.

Automated Z Calibration: Ground points per line were used to calculate the vertical divergence between lines caused by vertical GPS drift. Automated Z calibration was the final step employed for relative accuracy calibration.

Lidar accuracy error sources and solutions:

Source	Type	Post Processing Solution
Long Base Lines	GPS	None
Poor Satellite Constellation	GPS	None
Poor Antenna Visibility	GPS	Reduce Visibility Mask
Poor System Calibration	System	Recalibrate IMU and sensor offsets/settings
Inaccurate System	System	None
Poor Laser Timing	Laser Noise	None
Poor Laser Reception	Laser Noise	None
Poor Laser Power	Laser Noise	None
Irregular Laser Shape	Laser Noise	None

Operational measures taken to improve relative accuracy:

Low Flight Altitude: Terrain following was employed to maintain a constant above ground level (AGL). Laser horizontal errors are a function of flight altitude above ground (about 1/3000th AGL flight altitude).

Focus Laser Power at narrow beam footprint: A laser return must be received by the system above a power threshold to accurately record a measurement. The strength of the laser return (i.e., intensity) is a function of laser emission power, laser footprint, flight altitude and the reflectivity of the target. While surface reflectivity cannot be controlled, laser power can be increased and low flight altitudes can be maintained.

Reduced Scan Angle: Edge-of-scan data can become inaccurate. The scan angle was reduced to a maximum of $\pm 24.25^\circ$ from nadir, creating a narrow swath width and greatly reducing laser shadows from trees and buildings.

Quality GPS: Flights took place during optimal GPS conditions (e.g., 6 or more satellites and PDOP [Position Dilution of Precision] less than 3.0). Before each flight, the PDOP was determined for the survey day. During all flight times, a dual frequency DGPS base station recording at 1 second epochs was utilized and a maximum baseline length between the aircraft and the control points was less than 13 nm at all times.

Ground Survey: Ground survey point accuracy (<1.5 cm RMSE) occurs during optimal PDOP ranges and targets a minimal baseline distance of 4 miles between GPS rover and base. Robust statistics are, in part, a function of sample size (n) and distribution. Ground survey points are distributed to the extent possible throughout multiple flight lines and across the survey area.

50% Side-Lap (100% Overlap): Overlapping areas are optimized for relative accuracy testing. Laser shadowing is minimized to help increase target acquisition from multiple scan angles. Ideally, with a 50% side-lap, the nadir portion of one flight line coincides with the swath edge portion of overlapping flight lines. A minimum of 50% side-lap with terrain-followed acquisition prevents data gaps.

Opposing Flight Lines: All overlapping flight lines have opposing directions. Pitch, roll and heading errors are amplified by a factor of two relative to the adjacent flight line(s), making misalignments easier to detect and resolve.